

Topological momentum gap in PT-symmetric photonic crystals

Ming-Wei Li, Jian-Wei Liu, Wen-Jie Chen*, and Jian-Wen Dong*

*School of Physics & State Key Laboratory of Optoelectronic Materials and Technologies, Sun Yat-sen
University, Guangzhou 510275, China.*

*Corresponding author: chenwenj5@mail.sysu.edu.cn, dongjwen@mail.sysu.edu.cn

In a periodic system with parity-time (PT) symmetry, spontaneous breaking of PT symmetry occurs when non-Hermiticity exceeds a critical value, thereby dividing the Bloch bands into PT-exact phase and PT-broken phase in two momentum regimes. From another perspective, PT-broken momentum regime can be deemed as a momentum gap if we consider Bloch k as eigenvalue of the problem instead. The topological aspects of such a type of momentum gap (PT-broken regime) remain unexplored. Here, we study the topological properties of momentum bandgap in one-dimensional (1D) PT-symmetric photonic crystals (PCs). $k \cdot p$ analysis shows that reversing the system's non-Hermiticity would lead to a topological phase transition, which is manifested as a local geometric phase along the momentum band. As a consequence of such geometric phase, a temporal boundary state (TBS) exists in the middle of momentum gap. Its robustness against perturbations and disorders is numerically verified by temporal simulations.

The concept of parity-time (PT) symmetry and relevant non-Hermitian (NH) physics have drawn significant attention in many realms[1,2], from photonic to acoustic and mechanical systems[3-8], owing to the unique spectral features. Among them, photonic systems have been recognized as a convenient platform for studying the underlying physics and exploring their potential applications in optical devices[9-14]. By judiciously engineering the loss/gain profile of a periodic structure, photonic bands can exhibit entirely real eigenvalues in certain momentum regimes (termed as PT-exact phase) while forming complex conjugate pairs of the eigenvalues in other momentum regimes (PT-broken phase)[15-19]. At the phase transition momenta exist exceptional points (EPs, also known as branch singularities), where both eigenvalues and eigenvectors coalesce[20-23]. This exotic spectrum topology has been widely investigated and led to many novel phenomena dramatically different from Hermitian systems, such as coherent perfect absorption[24], unidirectional invisibility[25], laser mode selectivity[9], and asymmetric mode switching[26, 27].

In parallel with these developments, topological materials have revolutionized our understanding of boundary characteristic of a crystal, as they exhibit topologically robust physical phenomena immune to perturbation[28-31]. Relevant concepts and theories have been proposed and studied in Hermitian systems[32-34]. Since the eigenwavefunctions in NH systems have distinct properties from their Hermitian counterparts (such as nonorthogonality between wavefunctions), significant research efforts have been devoted to extending the topological concepts to NH systems[2, 21, 35-37]. Many intriguing effects have been revealed, including anomalous bulk-boundary correspondence[38], non-Hermitian skin effect[39], bulk Fermi arcs[40] and extended states outside continuum[41]. However, most of the previous works are concerned with the bulk topologies of energy/frequency bands and the associated in-gap spatial boundary states. In fact, PT-broken regimes in NH band structures can be

viewed as a momentum gap[42] if we consider Bloch k as the eigenvalue. The topological aspects of such type of momentum gap and its in-gap TBS are relatively unexplored.

In this paper, we investigate the topological properties of momentum bandgap in one-dimensional (1D) PT-symmetric systems. We begin with a simple two-band model by introducing an imaginary mass to 1D diabolic Hamiltonian. In its PT-broken momentum regime, the Hamiltonian takes the form of a momentum gap. The momentum bands separated by the gap are found to carry a local geometric phase, which depends on the sign of imaginary mass term. This indicates that an in-gap TBS should exist between the two PT systems with opposite masses. This idea is demonstrated using two 1D PT photonic crystals with opposite non-Hermiticities. Their distinct geometric phases are illustrated by tracing the eigenwavefunctions in a parallel transport process along the momentum bands. Moreover, the topologically protected boundary states are verified by numerical simulations and are shown to be robust against disorder or perturbation.

To illustrate our idea, we begin with a simple two-band model, written as $\hat{H}_\omega(k) = k\sigma_z$. It has a gapless dispersion with a linear band crossing at zone center, namely a diabolic point (orange sphere), as depicted in Fig. 1(b). Upon adding a real mass $m_R\sigma_y$ to the Hamiltonian: $\hat{H}_\omega(k) = m_R\sigma_y + k\sigma_z$, a frequency bandgap opens (Fig. 1(a)), which is commonly found in Hermitian system. Inside the band gap exist two branches of eigenmodes with real ω and complex k (orange lines in Fig.1(a)), which evanescently decay or grow in space. Interestingly, a real mass with positive or negative sign would lead to a topologically distinct frequency gap, expecting a protected interface mode localized at the domain wall between two systems with opposite masses[43]. Good examples are Su–Schrieffer–Heeger lattices and their high-dimensional counterparts. Notably, one can instead introduce an imaginary mass to the diabolical Hamiltonian, leading to a NH Hamiltonian:

$$\hat{H}_\omega(k) = im_l\sigma_y + k\sigma_z. \quad (1)$$

Inside the momentum regime ($-|m_l| < k < |m_l|$) resides two branches of eigenmodes with complex frequencies, as is common in NH systems with PT symmetry. Interestingly, the eigenvalue equation can be rewritten in the following form when momentum k is treated as an eigenvalue:

$$\hat{H}_k(\omega) = -m_l\sigma_x + \omega\sigma_z. \quad (2)$$

It takes a similar form as $\hat{H}_\omega(k) = m_R\sigma_y + k\sigma_z$, except that frequency ω and momentum k swap roles. In this regard, the PT-broken phase can be considered as a momentum gap. Furthermore, the complex frequency bands in the momentum gap correspond to the eigenmodes that would exponentially grow/decay with time. Then a natural question to ask is whether this momentum gap can exhibit nontrivial band topology. A recent work on photonic time crystals may provide some insights, although the momentum gap in the work was realized by a dynamical modulation on refractive index[42]. Here, we will show that even a simple PT-symmetric crystal can exhibit nontrivial band topologies, guaranteeing the existence of a TBS.

In principle, the ideas presented in this work should apply to any PT-symmetric or pseudo-Hermitian system[44]. For concreteness, we consider a 1D binary photonic crystal in Fig. 2(a). The dielectric constants of two-layered media are $\epsilon_1 = 1 - i\Gamma$ and $\epsilon_2 = 1 + i\Gamma$, where Γ represents the non-Hermiticity of the system. Without loss or gain ($\Gamma = 0$), the system is reduced to a homogeneous medium, and its dispersion is a light line $\omega = \frac{ck}{\sqrt{\epsilon_r}}$. As we assigned a periodicity of d , the light line folds forth and back between the Brillouin zone boundaries (BZBs). Fig. 2(e) plots the two lowest bands linearly crossing at BZB.

When the non-Hermiticity (Γ , with either positive or negative sign) is turned on, the diabolic point immediately splits into two EPs, producing a PT-broken regime (i.e., a momentum gap) in

between. Figs.2(d) and 2(g) exemplify the complex band structures for the crystal with $\Gamma = 0.2$. The unit cell is composed of a loss layer on top and a gain layer at the bottom (it is termed an LG crystal in the following discussion). Fig.2(f) and 2(i) show the case of a GL crystal with $\Gamma = -0.2$. As the time reversal counterpart of LG crystal, GL crystal has the same eigenspectrum as the LG crystal. Nevertheless, the eigenwavefunctions of the two crystals are different because of the swapping of the loss layer and the gain layer (see the eigenfields at two EPs in Figs. 2(d) and 2(f)). When Γ changes sign, the momentum gap closes and reopens, accompanied by the switching of the two-band edge states (two EP modes). The topologies of momentum bands change during this band inversion process. This can be interpreted by inspecting the effective Hamiltonian near the BZB.

To obtain the effective Dirac Hamiltonian[45], we begin with the following Helmholtz equation for a 1D PT crystal:

$$\left[\frac{d^2}{dz^2} + \left(\frac{\omega}{c} \right)^2 \varepsilon_r(z) \right] \psi(z, t) = 0 \quad . \quad (3)$$

Using two-plane wave approximation, an eigenmode around $k = \pi$ can be expanded as follows:

$$\psi(z, t) = A(\delta k) E_{+1} + B(\delta k) E_{-1}, \quad (4)$$

where $\delta k = k - \pi$ is the wavenumber deviated from the BZB, and $E_{+1} = e^{i[(\delta k + \pi)z - \omega t]}$ and $E_{-1} = e^{i[(\delta k - \pi)z - \omega t]}$ are the +1 and -1 terms of the Fourier series. $A(\delta k)$ and $B(\delta k)$ are the complex amplitudes of the two plane waves. After some algebra (see Supplemental Material S2), we obtain an effective Hamiltonian:

$$\hat{H}_\omega(\delta k) = \alpha \left(c_0 \sigma_0 - i m_\Gamma \sigma_y - c_3 \delta k \sigma_z \right), \quad (5)$$

where $m_\Gamma = \pi^2 \sqrt{\frac{\sqrt{\pi^2 + 4\Gamma^2} - \pi}{2\Gamma^2 \pi^2}} \Gamma$. Evidently, it takes a similar form as Eq. (1), where Γ introduces an imaginary mass. As presented in Fig. 2, a momentum band inversion occurs when the non-

Hermiticity (Γ) sign changes. For a 1D system, the band topology is typically characterized by Zak phase[46], which is the global geometric phase of eigenwavefunction along a closed path in parameter space. However, in our case, frequency (serving as a parameter) is not a cyclic parameter, and the Zak phase of a momentum band is not well-defined. Here, we investigate the local geometric phase near the momentum valley, similar to the valley Chern number in 2D valley Hall systems[47]. By rewriting the eigenvalue equation for frequency (see Supplemental Material S4), the momentum operator can be expressed as

$$\hat{H}_{\delta k}(\omega) = -\frac{1}{c_3} \left[\left(\frac{\omega}{\alpha} - c_0 \right) \sigma_z + m_\Gamma \sigma_x \right]. \quad (6)$$

Two eigenmomenta (δk) and the corresponding eigenvectors $|\psi_{\delta k}(\omega)\rangle$ reads

$$\delta k = \pm \frac{1}{c_3} \sqrt{m_\Gamma^2 + \left(\frac{\omega}{\alpha} - c_0 \right)^2}, \quad (7)$$

$$|\psi_{\delta k}(\omega)\rangle = \frac{1}{N_2} \begin{bmatrix} m_\Gamma \\ -\frac{\omega}{\alpha} + c_0 \pm \sqrt{m_\Gamma^2 + \left(\frac{\omega}{\alpha} - c_0 \right)^2} \end{bmatrix}, \quad (8)$$

where N_2 is a normalized coefficient. Here, we choose a parallel transport gauge.

Without loss of generality, we discuss the momentum band on the left side of the momentum gap ($\delta k < 0$). Owing to the lack of a closed parameter path in frequency, the geometric phase is ill-defined (gauge dependent). Therefore, we analyze the topological feature by comparing the local geometric phases between LG and GL systems[48] (i.e., a system with a positive imaginary mass and another system with a negative imaginary mass). From Eq. (8), it is easy to determine that the eigenvector at the high (low) frequency limit is always $[0, 1]^T$ ($[1, 0]^T$), regardless of the specific value of m_Γ . Thereafter, we adopt the eigenstate, $[1, 0]^T$, at low-frequency limit as the initial state to perform parallel transport, yielding a vanishing Berry connection everywhere on the momentum band. The

geometric phase is manifested by the phase of final state at high frequency limit, $[0,1]^T$ (see Supplemental Material S4). The phase of final state is 0 for positive m_T while is π for negative m_T . It implies that the topological feature of an LG crystal should be different from that of a GL crystal. Additionally, the closing and reopening of momentum gap (PT-broken regime) as Γ sign changes signify a topological phase transition[48].

Such a local geometric phase is verified by the simulated eigenmodes using the finite element method. Fig. 3 shows a plot of the eigen electric field in a unit cell for the LG crystal (left column) and the GL crystal (right column) shown in Fig. 2. Here, we adopt the eigenmodes at $0.3(2\pi c/d)$ as the initial states of the parallel transport for both crystals (yellow solid circles in Figs. 3(a) and 3(g). And an identical choice of initial phase is chosen for the two eigenmodes (they are parallel), as depicted in Figs. 3(f) and 3(l). Thereafter, we transport the two eigenmodes in a parallel manner along the left momentum bands, which requires the infinitesimal change in $|\psi_{\delta k}(\omega)\rangle$ to be orthogonal to itself. The two eigenmodes evolve as frequency increases, and the eigen fields at five representative frequencies are plotted in Figs. 3(b–f) and (h–l). We adopt the eigenmodes at $0.7(2\pi c/d)$ as the final states of parallel transport since it is sufficiently far from the momentum valley. As predicted by the effective Hamiltonian, the eigen fields of the two final states (Figs. 3(b) and (h)) take opposite signs, indicating that their local geometric phases are differentiated by π .

To clarify this evolution process, we add the corresponding two-component eigenvectors given by effective Hamiltonian (black arrows in colored circles) in the middle column of Fig.3. At the beginning of parallel transport, the eigenvectors for both systems are aligned in vertical direction. As frequency increases, the two eigenstates evolve into two different EP states at $0.4975(2\pi c/d)$, whose eigenvectors point to upper left or upper right direction. Then frequency further increases, the two

eigenvectors evolve to point in horizontal direction finally but to opposite sides (left and right), corresponding to the π phase difference. This is because of their different EP modes on the left momentum bands, attributed to the momentum band inversion (EP1 mode and EP2 mode swap their positions). Note that although we assume that the two crystals have opposite Γ in the above example, it is not a prerequisite. As long as the two systems under consideration have imaginary masses with opposite signs, their band topologies should be different.

Similar to the interface state between two topological distinct 1D crystals characterized by different Zak phases[42, 46], the distinct geometric phases of the LG and GL crystals lead to a TBS inside the momentum gap (see Supplemental Material S3). Suppose there is a 1D periodic LG crystal at the very beginning, then at some time point t_0 , each layer of the loss/gain medium simultaneously turns into a gain/loss medium (LG crystal becomes GL crystal). The electromagnetic wave amplitude would, at first, exponentially grow in the LG crystal before the transition and subsequently exponentially decay in the GL crystal after the transition, yielding a peak at transition time t_0 (see Fig. 4(a)). This process can be understood by the following dynamic equation based on the effective

Hamiltonian in Eq (5): $i \frac{\partial}{\partial t} |\psi(z, t)\rangle = \alpha (c_0 \sigma_0 - i m_{\Gamma}(t) \sigma_y - c_3 \delta k \sigma_z) |\psi(z, t)\rangle$, where

$$m_{\Gamma}(t) = \pi^2 \sqrt{\frac{\sqrt{\pi^6 + 4\Gamma^2 \pi^4} - \pi^3}{2\Gamma^2 \pi^4}} \Gamma(t), \text{ and } \Gamma(t) = 0.2 \text{step}(t - t_0)$$

is a step-like function indicating a sudden change in the imaginary mass. Thereafter, we find a solution at the midgap ($\delta k = 0$) with the wave function of

$$|\psi(z, t)\rangle = (A(0)e^{i\pi z} + B(0)e^{-i\pi z}) e^{-iac_0 t} e^{\alpha m_{\Gamma}(t)t}. \quad (9)$$

This TBS comprises a grow bulk mode in LG crystal ($m_{\Gamma}(t) > 0$) and a decay bulk mode in GL crystal ($m_{\Gamma}(t) < 0$). Fig. 4(b) shows the spatiotemporal profile given by full-wave simulation.

In the above discussions, the loss/gain profile of the system experiences a sudden change at transition time t_0 , as described by a step function. This is unrealistic and unphysical to some extent. Thus, we may ask is whether TBS can survive if the transition is smooth (for example, a sigmoid function).

In fact, the existence of TBS is not constrained to the case of a sharp, step-like transition. After analyzing the effective Hamiltonian around the momentum gap, one can prove that the edge state can be generalized to an almost arbitrary temporal dependence of the imaginary mass ($\Gamma(t)$) (see Supplemental Material S6). The only condition is that the sign of $\Gamma(t)$ changes in the two temporal domains, i.e., $\Gamma(t \rightarrow -\infty) > 0$ and $\Gamma(t \rightarrow \infty) < 0$. The wavefunction of TBS is written as

$$|\psi(z, t)\rangle \propto (A(0)e^{i\pi z} + B(0)e^{-i\pi z})e^{-iac_0 t} e^{\alpha \int^t dt' m_{\Gamma}(t')}. \quad (10)$$

Thus, a midgap TBS always exists as long as the two crystals are characterized by different geometric phases.

To verify this statement, three kinds of temporal boundaries are simulated in Fig. 5. First, a smooth variation in $\Gamma(t)$ is considered in Fig. 5(a), having the form of a sigmoid function:

$$S(t) = \frac{1}{1 + e^{-\frac{t-t_0}{4.4668 \times 10^{-10}}}} + 1. \quad \text{It is found that the temporal profile of electric field remains a localized peak}$$

near t_0 but varies in a relatively smooth manner. Secondly, we introduce disordered oscillation to $\Gamma(t)$ between the two crystals (from t_0 to t_1). As predicted by Eq. (10), the envelope function (dashed lines in Fig. 5(b)) first exponentially grows in LG crystal, then oscillates in the disordered medium following the variation of $\Gamma(t)$, and finally exponentially decays in GL crystal. In the third case, to demonstrate the ubiquitous existence of TBS between two topologically distinct crystals, a temporal boundary between the LG crystal ($\Gamma = 0.2$) and another G'L' crystal ($\Gamma = -0.3$) is simulated in Fig. 5(c). A localized temporal peak is still observed, except that the electric field decays faster in the G'L' crystal

than in Fig. 5(a).

In summary, we investigate the topological aspects of momentum bandgap in the simplest PT-symmetric photonic crystal. Further, $k \cdot p$ analysis shows that the PT crystals can possess distinct topological phases, depending on the non-Hermiticity sign. By bounding two topologically distinct PT crystals in time dimension, we find that a generic solution for the TBS is guaranteed by the topological phases. Such a type of TBS is numerically confirmed to be immune to perturbation and disorder. We believe that these findings would extend and supplement the current understanding of topological spatial edge states and provide new perspectives on topological physics in NH systems.

Acknowledgments

This work was supported by National Key R&D Program of China (Grant Nos. 2022YFA1404304, 2019YFA0706302), Guangdong Basic and Applied Basic Research Foundation (Grant No. 2023B1515040023).

REFERENCES

- [1] Ashida, Y., Z. P. Gong and M. Ueda, Non-Hermitian physics, *Advances in Physics* **69**, 249 (2020).
- [2] El-Ganainy, R., K. G. Makris, M. Khajavikhan, Z. H. Musslimani, S. Rotter and D. N. Christodoulides, Non-Hermitian physics and PT symmetry, *Nat. Phys.* **14**, 11 (2018).
- [3] Bender, C. M., B. K. Berntson, D. Parker and E. Samuel, Observation of PT phase transition in a simple mechanical system, *American Journal of Physics* **81**, 173 (2013).
- [4] Fleury, R., D. Sounas and A. Alù, An invisible acoustic sensor based on parity-time symmetry, *Nat. Commun.* **6**, 5905 (2015).
- [5] Hu, B., Z. Zhang, H. Zhang, L. Zheng, W. Xiong, Z. Yue, X. Wang, J. Xu, Y. Cheng, X. Liu and J. Christensen, Non-Hermitian topological whispering gallery, *Nature* **597**, 655 (2021).
- [6] Liu, Y., T. Hao, W. Li, J. Capmany, N. Zhu and M. Li, Observation of parity-time symmetry in microwave photonics, *Light Sci Appl* **7**, 38 (2018).

- [7] Mao, X., G.-Q. Qin, H. Yang, H. Zhang, M. Wang and G.-L. Long, Enhanced sensitivity of optical gyroscope in a mechanical parity-time-symmetric system based on exceptional point, *New J. Phys.* **22**, 093009 (2020).
- [8] Rüter, C. E., K. G. Makris, R. El-Ganainy, D. N. Christodoulides, M. Segev and D. Kip, Observation of parity-time symmetry in optics, *Nat. Phys.* **6**, 192 (2010).
- [9] Feng, L., Z. J. Wong, R.-M. Ma, Y. Wang and X. Zhang, Single-mode laser by parity-time symmetry breaking, *Nature* **346**, 972 (2014).
- [10] K. G. Makris, R. E.-G., and D. N. Christodoulides, Beam dynamics in PT symmetric optical lattices, *Phys. Rev. Lett.* **100**, 103904 (2008).
- [11] Lin, Z., H. Ramezani, T. Eichelkraut, T. Kottos, H. Cao and D. N. Christodoulides, Unidirectional invisibility induced by PT-symmetric periodic structures, *Phys. Rev. Lett.* **106**, 213901 (2011).
- [12] Longhi, S., Parity-time symmetry meets photonics: A new twist in non-Hermitian optics, *Europhysics Letters* **120**, 64001 (2017).
- [13] Sakhdari, M., M. Farhat and P.-Y. Chen, PT-symmetric metasurfaces: wave manipulation and sensing using singular points, *New J. Phys.* **19**, 065002 (2017).
- [14] Xia, S. Q., D. Kaltsas, D. H. Song, I. Komis, J. J. Xu, A. Szameit, H. Buljan, K. G. Makris and Z. G. Chen, Nonlinear tuning of PT symmetry and non-Hermitian topological states, *Science* **372**, 72-+ (2021).
- [15] Bender, C. M. and S. Boettcher, Real spectra in nonHermitian Hamiltonians having PT Symmetry, *Phys. Rev. Lett.* **80**, 5243 (1998).
- [16] Bittner, S., B. Dietz, U. Gunther, H. L. Harney, M. Miski-Oglu, A. Richter and F. Schafer, PT Symmetry and Spontaneous Symmetry Breaking in a Microwave Billiard, *Physical Review Letters* **108** (2012).
- [17] Guo, A., G. J. Salamo, D. Duchesne, R. Morandotti, M. Volatier-Ravat, V. Aimez, G. A. Siviloglou and D. N. Christodoulides, Observation of PT-Symmetry Breaking in Complex Optical Potentials, *Physical Review Letters* **103** (2009).
- [18] Levai, G. and M. Znojil, Systematic search for PT-symmetric potentials with real energy spectra, *J. Phys. A: Math. Gen.* **33**, 7165 (2000).
- [19] R. El-Ganainy, K. G. M., D. N. Christodoulides and Ziad H. Musslimani, Theory of coupled optical PT-symmetric structures, *Opt. Lett.* **32**, 2632 (2007).

- [20] Bergholtz, E. J., J. C. Budich and F. K. Kunst, Exceptional topology of non-Hermitian systems, *Rev. Mod. Phys.* **93**, 015005 (2021).
- [21] Ding, K., C. Fang and G. Ma, Non-Hermitian topology and exceptional-point geometries, *Nat. Rev. Phys.* **4**, 745 (2022).
- [22] Parto, M., Y. G. N. Liu, B. Bahari, M. Khajavikhan and D. N. Christodoulides, Non-Hermitian and topological photonics: optics at an exceptional point, *Nanophotonics* **10**, 403 (2021).
- [23] Zhen, B., C. W. Hsu, Y. Igarashi, L. Lu, I. Kaminer, A. Pick, S. L. Chua, J. D. Joannopoulos and M. Soljačić, Spawning rings of exceptional points out of Dirac cones, *Nature* **525**, 354 (2015).
- [24] Wang, C. Q., W. R. Sweeney, A. D. Stone and L. Yang, Coherent perfect absorption at an exceptional point, *Science* **373**, 1261 (2021).
- [25] Feng, L., Y. L. Xu, W. S. Fegadolli, M. H. Lu, J. E. Oliveira, V. R. Almeida, Y. F. Chen and A. Scherer, Experimental demonstration of a unidirectional reflectionless parity-time metamaterial at optical frequencies, *Nat. Mater.* **12**, 108 (2013).
- [26] Doppler, J., A. A. Mailybaev, J. Bohm, U. Kuhl, A. Girschik, F. Libisch, T. J. Milburn, P. Rabl, N. Moiseyev and S. Rotter, Dynamically encircling an exceptional point for asymmetric mode switching, *Nature* **537**, 76 (2016).
- [27] Xu, H., D. Mason, L. Y. Jiang and J. G. E. Harris, Topological energy transfer in an optomechanical system with exceptional points, *Nature* **537**, 80 (2016).
- [28] Haldane, F. D. M. and S. Raghu, Possible Realization of Directional Optical Waveguides in Photonic Crystals with Broken Time-Reversal Symmetry, *Physical Review Letters* **100**, 013904 (2008).
- [29] Raghu, S. and F. D. M. Haldane, Analogs of quantum-Hall-effect edge states in photonic crystals, *Physical Review A* **78**, 033834 (2008).
- [30] Wang, Z., Y. Chong, J. D. Joannopoulos and M. Soljačić, Observation of unidirectional backscattering-immune topological electromagnetic states, *Nature* **461**, 772-775 (2009).
- [31] Wang, Z., Y. D. Chong, J. D. Joannopoulos and M. Soljačić, Reflection-Free One-Way Edge Modes in a Gyromagnetic Photonic Crystal, *Physical Review Letters* **100**, 013905 (2008).
- [32] Ma, G., M. Xiao and C. T. Chan, Topological phases in acoustic and mechanical systems, *Nat. Rev. Phys.* **1**, 281 (2019).
- [33] Ozawa, T., H. M. Price, A. Amo, N. Goldman, M. Hafezi, L. Lu, M. C. Rechtsman, D. Schuster, J.

- Simon, O. Zilberberg and I. Carusotto, Topological photonics, *Rev. Mod. Phys.* **91**, 015006 (2019).
- [34] Tang, G. J., X. T. He, F. L. Shi, J. W. Liu, X. D. Chen and J. W. Dong, Topological Photonic Crystals: Physics, Designs, and Applications, *Laser & Photonics Reviews* **16** (2022).
- [35] Ghatak, A. and T. Das, New topological invariants in non-Hermitian systems, *J. Phys.: Condens. Matter* **31**, 263001 (2019).
- [36] Kawabata, K., K. Shiozaki, M. Ueda and M. Sato, Symmetry and Topology in Non-Hermitian Physics, *Phys Rev. X* **9**, 041015 (2019).
- [37] Wang, H., X. Zhang, J. Hua, D. Lei, M. Lu and Y. Chen, Topological physics of non-Hermitian optics and photonics: a review, *J. Opt.* **23**, 123001 (2021).
- [38] Lee, T. E., Anomalous Edge State in a Non-Hermitian Lattice, *Phys. Rev. Lett.* **116**, 133903 (2016).
- [39] Yao, S. and Z. Wang, Edge States and Topological Invariants of Non-Hermitian Systems, *Physical Review Letters* **121**, 086803 (2018).
- [40] Zhou, H. Y., C. Peng, Y. Yoon, C. W. Hsu, K. A. Nelson, L. Fu, J. D. Joannopoulos, M. Soljacic and B. Zhen, Observation of bulk Fermi arc and polarization half charge from paired exceptional points, *Science* **359**, 1009 (2018).
- [41] Wang, W., X. Wang and G. Ma, Extended State in a Localized Continuum, *Physical Review Letters* **129**, 264301 (2022).
- [42] Lustig, E., Y. Sharabi and M. Segev, Topological aspects of photonic time crystals, *Optica* **5** (2018).
- [43] János K. Asbóth, L. O., András Pályi, *A Short Course on topological insulator*. (2015).
- [44] Mostafazadeh, A., Pseudo-Hermiticity versus PT symmetry: The necessary condition for the reality of the spectrum of a non-Hermitian Hamiltonian, *Journal of Mathematical Physics* **43**, 205-214 (2002).
- [45] Ding, K., Z. Q. Zhang and C. T. Chan, Coalescence of exceptional points and phase diagrams for one-dimensional PT-symmetric photonic crystals, *Phys. Rev. B.* **92** (2015).
- [46] Xiao, M., Z. Q. Zhang and C. T. Chan, Surface Impedance and Bulk Band Geometric Phases in One-Dimensional Systems, *Phys. Rev. X.* **4**, 021017 (2014).
- [47] Liu, J.-W., F.-L. Shi, X.-T. He, G.-J. Tang, W.-J. Chen, X.-D. Chen and J.-W. Dong, Valley photonic crystals, *Advances in Physics: X* **6**, 1905546 (2021).

[48] Raffaele, R., Manifestations of Berry's phase in molecules and condensed matter, J. Phys.: Condens. Matter **12**, R107 (2000).

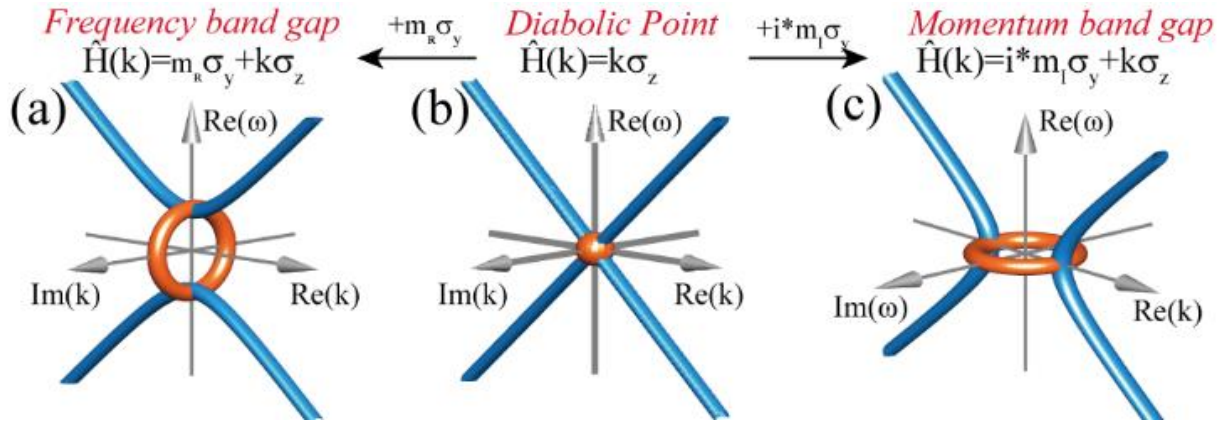


FIG. 1. Frequency bandgap and momentum bandgap in 1D system. (a) Frequency bandgap by adding real mass. Inside the gap are two branches of evanescent modes (orange lines) that exponentially decay/grow in space. (b) 1D dispersion with a diabolic point. Two bulk bands (blue) linearly cross at a k -point (orange sphere), whose physics can be well captured by the Hamiltonian of $\hat{H}_\omega(k) = k\sigma_z$. Upon adding a real (imaginary) mass to the diabolic Hamiltonian, a frequency (momentum) gap will open at the crossing point. (c) Momentum bandgap by adding imaginary mass. Inside the gap are two branches of unstable modes (orange lines) that exponentially decay/grow with time.

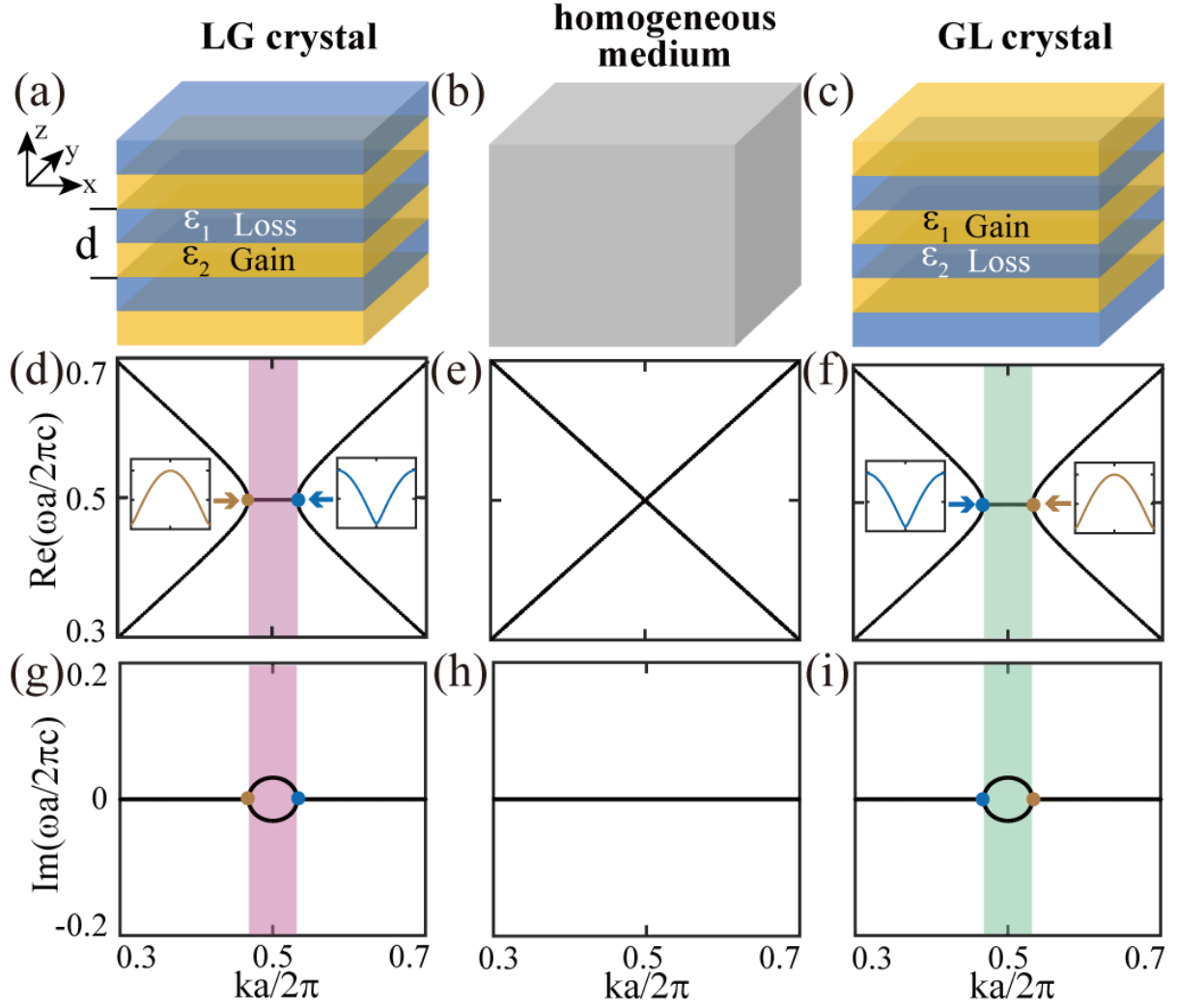


FIG. 2. Topological momentum gaps in the 1D PT-symmetric photonic crystals. The system under consideration is a binary PC with the system parameters: $d_1 = d_2 = 0.5d$, $\epsilon_1 = 1 - i\Gamma$, $\epsilon_2 = 1 + i\Gamma$, and $\mu_1 = \mu_2 = 1$. When $\Gamma = 0$, the system is reduced to a homogeneous medium (vacuum). The lowest two bands linearly cross at BZB (middle column). When loss and gain are turned on ($\Gamma \neq 0$), the two bands mix and merge, generating a PT-broken regime between two EPs (brown and blue circles). (a) 1D PT crystal with $\Gamma = 0.2$, namely an LG crystal. (d) & (g) Corresponding complex band structure. (b) Homogeneous medium with $\Gamma = 0$. (e) & (h) Corresponding band structure. (c) 1D PT crystal with $\Gamma = -0.2$, namely a GL crystal. (f) & (i) Corresponding complex band structure. As the non-Hermiticity Γ decreases and changes sign, the system experiences a topological phase transition. The momentum gap closes and reopens, along with the two EP modes swapping their positions [insets of (d) and (f)].

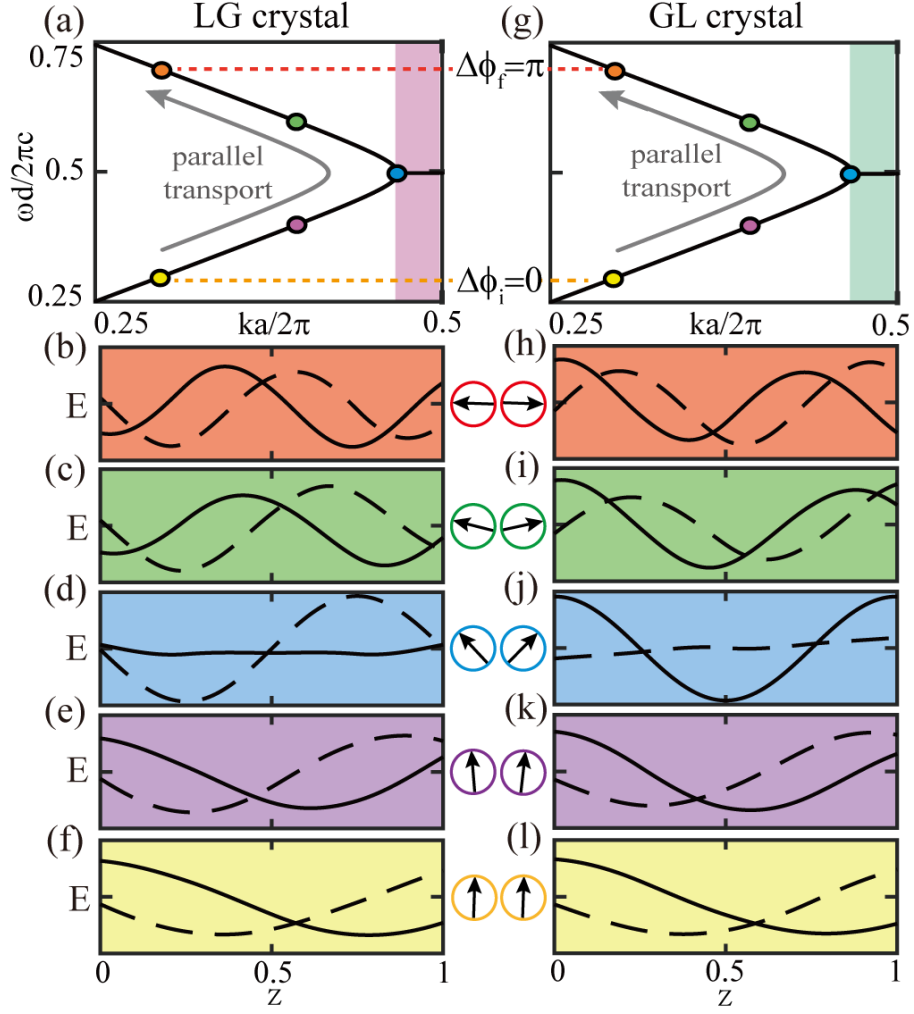


FIG. 3. Parallel transport of the eigenwavefunctions along the momentum bands. (a) & (g) Real band structures of the considered momentum bands (on the left of momentum gap) for LG and GL crystals. (b–f) Eigen electric fields at five representative frequencies for LG crystal. Solid lines and dash lines represent the real and imaginary part of the eigen electric fields. (h–l) Eigen electric fields for GL crystal. The gray arrows in (a) and (g) indicate the directions of parallel transport. The two eigenwavefunctions at frequency of $0.3(2\pi c/d)$ (yellow circles) are chosen as the initial states of parallel transport, for which we assign the same initial phase [(f) and (l)]. Using parallel transport gauge, we find that the final states in (b) and (h) accumulate a phase difference of π , as predicted by the eigenvectors of effective Hamiltonians [arrows in (b–l)]. This indicates the distinct band topologies of momentum bands in the two crystals.

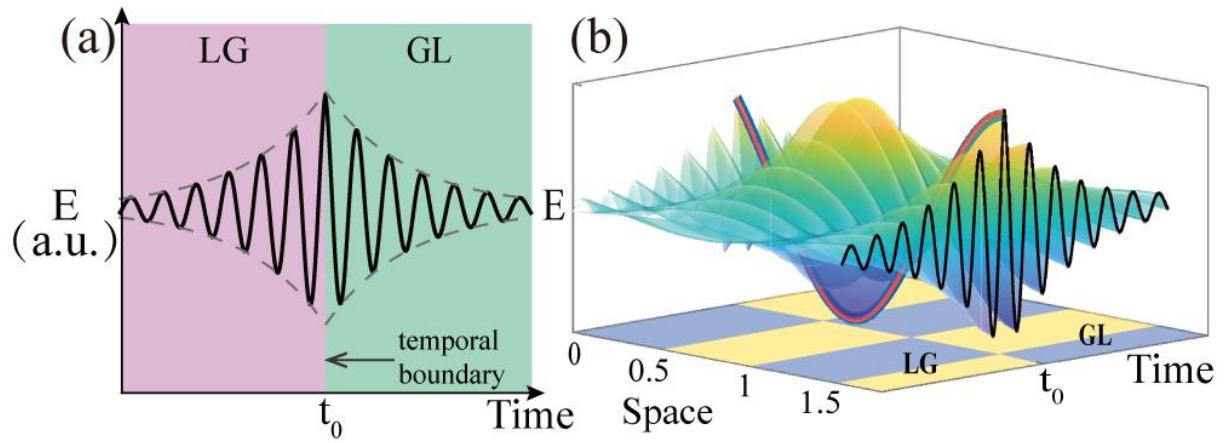


FIG. 4. TBS between LG and GL crystals. (a) Temporal boundary between LG crystal and GL crystal, where the system is switched from LG to GL at time t_0 . A TBS is localized near the temporal boundary at t_0 , which comprises the midgap growth mode in LG crystal ($t < t_0$) and the midgap decay mode in GL crystal ($t > t_0$). (b) Spatiotemporal profile of the TBS.

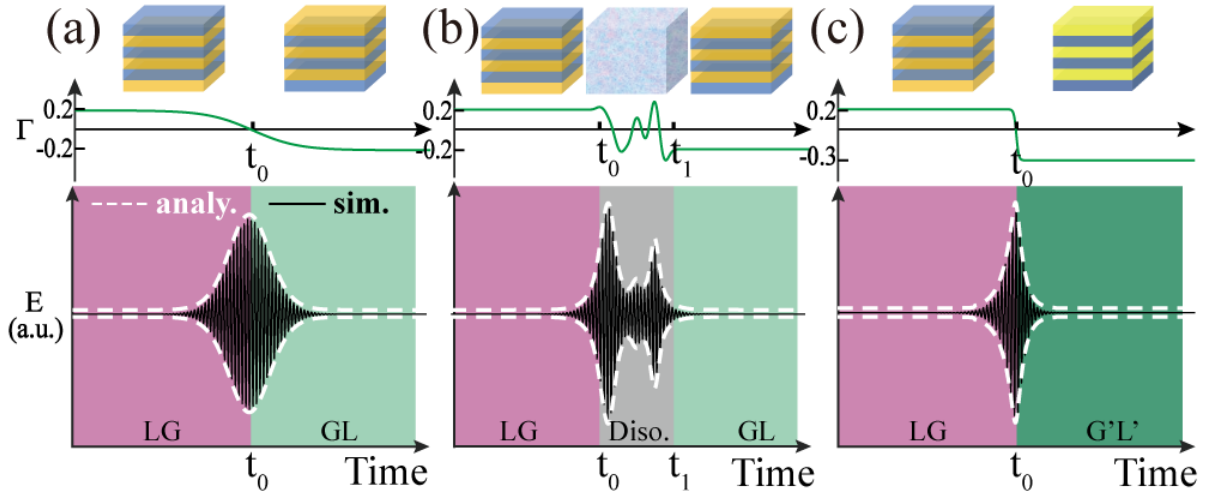


FIG. 5. Robust boundary states between two topologically distinct PT crystals. To demonstrate the ubiquitous existence of TBS, we simulate three cases of temporal boundaries. (a) Temporal boundary between LG crystal ($\Gamma = 0.2$) and GL crystal ($\Gamma = -0.2$) with a smooth variation in Γ . (b) Temporal boundary with a disordered variation of Γ in between the two crystals. (c) Temporal boundary between LG crystal ($\Gamma = 0.2$) and another L'G' crystal ($\Gamma = -0.3$), where the two crystals are no longer related by time reversal. The upper panels in (a)–(c) sketch the considered temporal process, whereas the lower panels plot the simulated electric field at position $z = 0$.